

NANO-ONIONS BASED ON CHITOSAN: PRODUCTION AND CHARACTERIZATION

Nanocebollas a base de quitosano: producción y caracterización

Yedidia VILLEGAS-PERALTA, Reyna G. SÁNCHEZ-DUARTE*, Jaime LÓPEZ-CERVANTES,
Dalia I. SÁNCHEZ-MACHADO, María del Rosario MARTÍNEZ-MACÍAS,
Nidia Josefina RÍOS-VÁZQUEZ, Germán Eduardo DÉVORA-ISIORDIA
and Ma. Araceli CORREA-MURRIETA

Instituto Tecnológico de Sonora, 5 de Febrero 818 Sur, 85000 Ciudad Obregón, Sonora, México.

*Author for correspondence: reyna.sanchez@itson.edu.mx

(Received: December 2020; Accepted: August 2022)

Key words: nanotubes, adsorbent, nanocomposite, lecithin, shrimp waste.

ABSTRACT

This work presents the morphology and characterization of chitosan nanoparticles crosslinked with lecithin in the form of nano-onions obtained by an easy, economical, and possibly scalable method from a polymeric precursor known as chitosan. The creation of new products by using shrimp waste is a fundamental factor in avoiding water pollution. These materials have a positive impact as they add value to waste, and they provide the opportunity to decrease pollution. Chitosan nano-onions were synthesized by an environmentally friendly, easy, and inexpensive method using chitosan as a natural source. Chitosan nano-onions (CSNO) were characterized by using Fourier transform infrared spectroscopy (FTIR), X-ray diffraction (XRD), scanning electron microscopy (SEM), transmission electron microscopy (TEM), dynamic light scattering (DLS) and specific surface area (SSA). The nano-onions characterization obtained by FTIR shows the presence of carbonyl groups at a wavenumber of 1752.12 cm^{-1} , while the phosphate groups attributed to lecithin are observed at 1156.88 cm^{-1} . XRD analysis confirmed an amorphous structure, while SEM images presented a globular morphology with concave surfaces. TEM analysis showed that the nano-onions are congregated in a unique structure that includes nanotubes. The CSNO average diameter by DLS was 442.5 nm with an octagonal arrangement, and a polydispersity index (PDI) of 0.532 and 31.9 mV . The average size of CSNO, the PDI, and the value of zeta potential were indicators of a stable dispersion with a specific superficial area measured by the Brunauer-Emmett-Teller (BET) method of $1.4\text{ m}^2\text{ g}^{-1}$. The results of the chitosan-lecithin nano-onions characterization indicate changes in the surface of the material with a larger total surface area and pore structure, compared to that of pure chitosan. According to the results of the CHNO characterization, they could be used as adsorbents for contaminants and they also have a potential application in the biomedical area, mainly as drug encapsulation material.

Palabras clave: nanotubos, adsorbente, nanocompuestos, lecitina, residuos de camarón.

RESUMEN

Este trabajo presenta la morfología y caracterización de nanopartículas de quitosano entrecruzadas con lecitina en forma de nanocebollas obtenidas a partir de un proceso sencillo, económico y escalable a partir de un polímero precursor como es el quitosano. La creación de nuevos productos mediante el uso de desechos de camarón es un factor fundamental para evitar la contaminación del agua. Estos materiales tienen un impacto positivo al agregar valor a los desechos y brindan la oportunidad de disminuir la contaminación. La síntesis de nanocebollas de quitosano se logró con un método amigable con el medio ambiente, sencillo y económico, utilizando quitosano como fuente natural. Las nanocebollas de quitosano (CSNO, por su sigla en inglés) se caracterizaron por espectroscopía infrarroja por transformada de Fourier (FTIR), difracción de rayos X (XRD), microscopía electrónica de barrido (SEM), microscopía electrónica de transmisión (TEM), dispersión dinámica de luz (DLS) y área superficial específica (SSA). La caracterización de las nanocebollas obtenidas mediante FTIR muestra la presencia de grupos carbonilo a un número de onda de 1752.12 cm^{-1} , mientras que los grupos fosfato atribuidos a la lecitina se observan a 1156.88 cm^{-1} . El análisis XRD confirmó una estructura amorfa, mientras que las imágenes SEM presentaron una morfología globular con superficies cóncavas. El análisis TEM mostró que las nanocebollas se congregan en una estructura única que incluye nanotubos. El diámetro promedio de las CSNO por DLS fue de 442.5 nm con una disposición octagonal, un índice de polidispersión (PDI) de 0.532 y 31.9 mV. El tamaño promedio de las CSNO, el PDI y el valor del potencial zeta fueron indicadores de una dispersión estable con un área superficial específica (SSA) medida por el método Brunauer-Emmett-Teller (BET) de $1.4\text{ m}^2\text{ g}^{-1}$. Los resultados de la caracterización de nanocebollas de quitosano-lecitina indican cambios en la superficie del material con un área superficial total más grande y estructura de poros, en comparación con la de quitosano puro. De acuerdo con los resultados de la caracterización de las CSNO, éstas podrían usarse como adsorbentes de contaminantes y tienen aplicación potencial en el área biomédica, principalmente como material de encapsulación de medicamentos.

INTRODUCTION

The use of nanomaterials is of great interest for their study due to their size and the applications they can have thanks to the physical and chemical properties, which they acquire at the nanometric scale compared to micro-sized material. Among these nanomaterials, chitosan nanoparticles are of great interest since they are obtained thanks to the versatility of chitosan and availability of functional groups (amino, $-\text{NH}_2$), non-toxicity, biocompatibility, and biodegradability (Divya et al. 2019). In the last two decades, nanotechnology has emerged significantly with its applications in almost all branches of science and technology (Magnuson et al. 2011, Santhosh et al. 2016). It has given a great impulse for the development and functionality of new materials. Nanostructures have been developed for pharmaceutical and biomedical industries, in which nanomaterials are used as drug delivery vehicles (Shi et al. 2010) and nano-formulations for oncology (Lin 2015). They also have been used in agricultural production, animal feed, food processing, additives, and food contact materials (Peters et al. 2016); in medicine as

biosensors and drug delivery (Yousfan et al. 2020), and for wastewater treatment as adsorbents, coagulants and flocculent (de Toledo et al. 2021).

The search for new materials that remove specific pollutants from water is the current trend in science. A good example is the production of carbon nano-onions, which are part of the chemistry family of fullerenes. They are formed of quasi-spherical-and polyhedral-shaped graphite layers with an interplanar distance of 0.335 nm (Suárez-Martínez et al. 2012). These adsorbents have attracted plentiful research interest for their adsorbing properties to the movement of ions (Singh 2018), high superficial area, and mechanical strength (Plonska-Brzezinska 2019).

Several methods have been reported for the synthesis of carbon nano-onions; however, these methods are not used to obtain chitosan nano-onions (CSNO) because high temperatures, inert atmospheres, high pressures or vacuums, and high voltage and current, are required (Mykhailiv et al. 2017). Substrates frequently used to generate carbon nano-onions are carbon soot, methane, propane and plastic wastes, as well as natural sources as lycopene from tomatoes (Singh 2018). Nowadays an attractive, promising, and

environmentally friendly natural source to produce nano-onions is chitosan, a cationic polysaccharide obtained by the N-deacetylation of chitin, a product found in the shells of crustaceans. Chitosan has been investigated in reference to the production of nanoparticles and stabilization of microemulsions due to its biocompatibility, null toxicity, biodegradability, and high potential to adsorb pollutants from water (Dou et al. 2019). However, to increase the stability of carbon nano-onions from chitosan, a mixture of lipids (lecithin) is commonly used. Lecithin interacts with the negative charge of its hydrophilic part and helps to form the core of nanostructures (Valencia et al. 2021).

Among the various polymers that can be used in the development of nanoparticles, we highlight chitosan, a linear cationic polysaccharide. The production of nanoparticles from chitosan has been extensively studied, but little is known about obtaining CSNO. Knowledge about the chitosan matrix complex to form nano-onions is currently being explored. Amiri et al. (2016) prepared carbon nitride/chitosan graphitic compounds by pyrolysis for adsorption and electrochemical determination of mercury in real samples; Abd et al. (2019) synthesized and characterized chitosan/polyacrylic acid/copper nanocomposites and described their impact on onion production, and Guo et al. (2019) elaborated carbon nanotube-grafted chitosan by the graphitization method.

In this context, there is little information on methods for obtaining CSNO and their characterization. Therefore, the objective of this work is the synthesis and characterization of chitosan-lecithin nano-onions by ionic gelation (a new production method) using chitosan as a natural and environmentally friendly source without the application of complex technology for its production. These nano-onions could be used as adsorbents of pollutants present in aqueous solutions. Also, lecithin-nanoparticles coated with chitosan are examples of nanocarriers of bioactive compounds (or other active substances) for numerous applications due to their numerous advantages, such as improving the physical-chemical stability, controlling the release of the compound, improving the activity of antimicrobials, and increasing the bioavailability and effectiveness of the compound (Frank et al. 2020).

MATERIALS AND METHODS

Materials

Sodium hydroxide (NaOH) reagent grade, 97 %; sodium tripolyphosphate (TPP) reagent grade, 85 %, purchased from Sigma-Aldrich (Saint Louis MO,

USA); hydrochloric acid (HCl) analytical grade, 97 %, purchased from Faga Lab, Monterrey Mexico; commercial soy lecithin and noncommercial chitosan produced from shrimp shells in the biopolymers laboratory of the Centro de Investigación e Innovación Biotecnológica, Agropecuaria y Ambiental, Instituto Tecnológico de Sonora. Deionized water was utilized for the preparations of all solutions. Chemicals were used without any further purification.

Chitosan production

The synthesis of CSNO concerns the use of non-commercial chitosan produced from shrimp wastes at laboratory by following the method of Sánchez-Duarte et al. (2012). These processes involve three steps: demineralization, deproteinization, and deacetylation of the shell. Briefly, in demineralization the shrimp shell was placed in a solution of 1 M HCl (1:10 m/v) and stirred mechanically for 4 h at room temperature. Next in the deproteinization, the shrimp shell in a 4.5 % NaOH solution (1:15 m/v) was mechanically stirred at 65 °C in an oil bath for 4 h. Finally, in deacetylation, the shell is mechanically stirred in a solution of 45 % NaOH at 110 °C in an oil bath for 2 h. After each step, the samples were washed with water until they reached a pH of 7. The chitosan obtained was used for the production of nano-onions.

Production of chitosan nano-onions

The noncommercial chitosan, sodium tripolyphosphate (TPP), and soy lecithin were applied in the procedure of Villegas-Peralta et al. (2019) to CSNO production. The chitosan of deacetylation degree, 92.16 %, was solubilized in of acetic acid. The chitosan solution was filtered to eliminate impurities. Granular soy lecithin was diluted in ethanol ($\text{CH}_3\text{CH}_2\text{OH}$, 98 %) to a concentration of 5 % (w/v). TPP was used to prepare a 0.14 % (w/v) solution. The lecithin solution was dropped immediately after the TPP solution was added drop-wise at a constant rate. All of the above were processed under contact magnetic stirring. Once lecithin and TPP finished dripping, the solution was stirred for 20 min. After a period of freezing, the solution was stirred. For the purification of the sample, a wash was made with distilled water, and then it was centrifuged for 40 min. The solid was separated and two more 20-min washes were performed. The solid phase was separated by centrifugation and then it was lyophilized to make the corresponding characterization.

Characterization of chitosan nano-onions

A Fourier transform infrared (FTIR) spectrometer (Thermo Scientific Spectrum model Nicolet iS5) was

used to identify the functional groups of the samples with an iD1 accessory of transmission. Previously to the analysis of the samples, they were dried at 40 °C overnight. A KBr pellet was used to record FTIR spectra in a range of 4000 to 400 cm⁻¹, with a resolution of 4 cm⁻¹. The weight relation of the sample and the KBr preparation (in g) was 0.02:0.45, respectively. OMNIC software was used to identify the functional groups.

The phase composition and crystallinity of the samples were analyzed using a Philips X'pert MPD (XRD) X-ray diffractometer. X-ray diffraction patterns were recorded in the range of 5° to 60° (2θ), with a step size of 0.05°. The equipment was used under a radiation of 40kV and 45 mA.

The morphology of CSNO was investigated by scanning electron microscopy (SEM) (model JEOL JSM-5300) at 10 kV, coupled to an energy-dispersive X-ray spectrophotometer (EDS) used to verify the elements in each sample. Magnifications of 2000X were used. The samples in solid stated were placed on a carbon base.

The CSNO size was examined by using a transmission electron microscope (TEM, JEOL JEM-2010 at 200 kV) and dynamic light scattering (DLS) with a Zetasizer Nano ZS (Malvern Instruments). The preparation of the sample for DLS and TEM was the same. Firstly, the sample was suspended in water and then it was sonicated for 10 min. To analyze the samples, they were placed in a cooper grid (Lacey carbon, SPI supplies) and in a glass cell (10 × 10 mm) for TEM and DLS, respectively. Additionally, the polydispersity index (PDI) value and zeta potential were analyzed using a ZEN-1102 zeta dip cell. The measures were expressed as mean ± standard deviation.

With a drying time and temperature of 12 h and 40 °C, respectively, a sample of 2.5 g was conditioned to determine the specific surface area using an advanced micropore size and chemisorption analyzer (Quanta-chrome Autosorb-iQ-C, USA). The Brunauer-Emmett-Teller (BET) nitrogen adsorption method was applied.

RESULTS AND DISCUSSION

CSNO mechanism of formation

Under acidic conditions, the crosslinking process between TPP and chitosan was improved due to the excess of ions produced by the protonation of more amino groups of chitosan ($pK_a < 6.3$), which interact with negative charges of phosphatesgroups of TPP and lecithin ($pK_a < 3$). During the formation of chitosan-TPP nanoparticles, a solution formed by alcohol and lecithin was incorporated as a coat. The nanosystem

was spontaneously assembled as nano-onions by a solvent displacement, the alcohol (solvent) was mixed in the organic phase migrating to the aqueous phase and the lecithin acted as stabilizer adsorbed in the interphase (Goycoolea et al. 2012). After a few minutes of stirring the formation of aggregates was observed. Due to its hydrophilic condition, lecithin forms negatively charged layers on the surfaces of certain compounds, in this case, chitosan (Fig. 1). Some authors (e.g., Mattu et al. 2013) suggest that proteins will rather be adsorbed on the particle surface than being entrapped inside, a behavior that can be observed in TEM analysis and is similar to the one reported by Kwamman et al. (2016). Another suggestion is that lecithin helps to form the outer layer of the chitosan nano-onions (Tran et al. 2015). Assembled nanoparticles are useful for encapsulating hydrophilic groups of different compounds, which is another confirmation of the acquired form of chitosan nano-onions.

In its bulk form, chitosan offers limited applications as adsorbent in water treatment, hence the reason why a new material (CSNO) is required to be characterized. Accordingly, the results of these techniques' characterizations are described below.

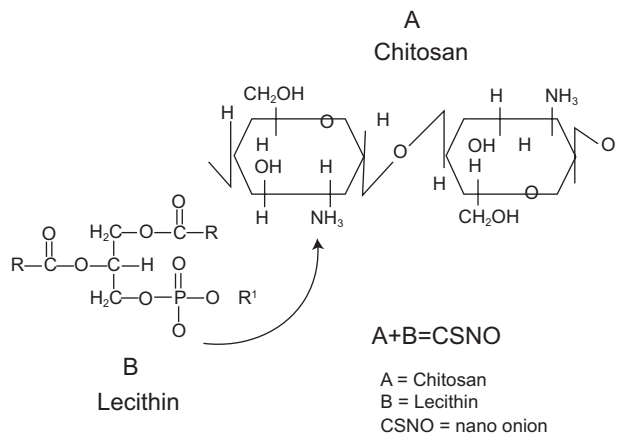


Fig. 1. Crosslinking reaction between chitosan and lecithin for the formation of chitosan nano-onions (CSNO).

Fourier transform infrared spectroscopy

FTIR was used to identify the chemical structure of chitosan, and the interactions with cross-linking agents (Stoica-Guzun et al. 2010) is a way to confirm the crosslinking between chitosan, lecithin and TPP. The FTIR information of chitosan nano-onions is shown in figure 2. The FTIR technique revealed the infrared spectrum of the interactions between functional groups of the lipid (lecithin) and

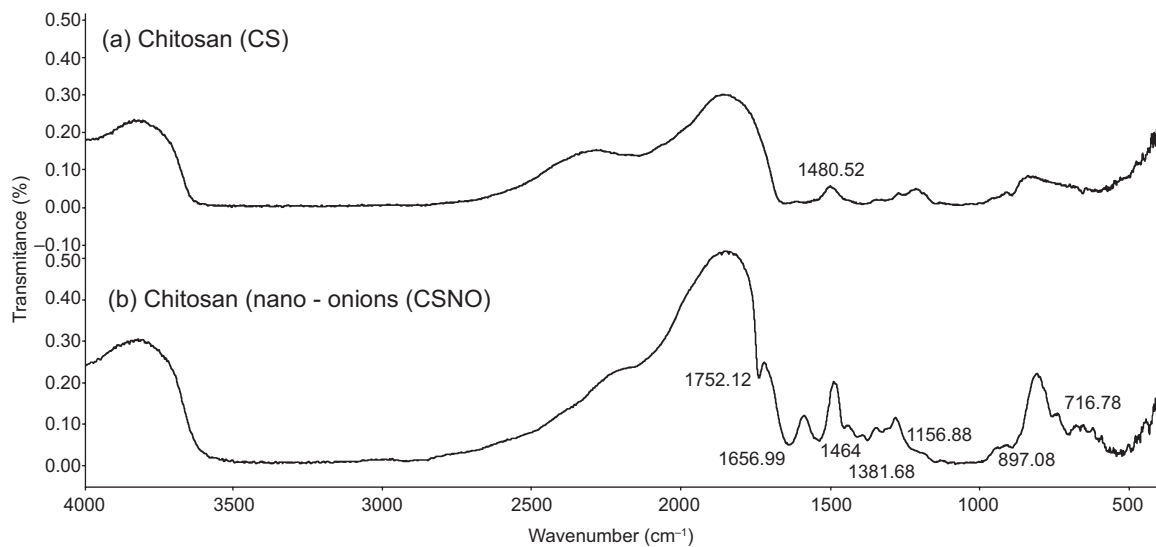


Fig. 2. Fourier transform infrared spectra of (a) raw chitosan (CS) and (b) chitosan nano-onions (CSNO).

chitosan. Commonly, chitosan from shrimp wastes presents an NH_2 vibration of primary amino at 1590 cm^{-1} (Sonvico et al. 2006, Wang et al. 2011). In this work it appeared with a light displacement at 1546.32 cm^{-1} . A typical absorption of the nanosystem formed by a lecithin and chitosan band was current at 1752.12 cm^{-1} due to the stretching of the carbonyl groups of the fatty acids. Characteristic peaks of unites of chitosan glucosamine were observed at 1656.99 cm^{-1} (Souza et al. 2014). Chitosan nano-onions were produced due to the self-organizing interaction of positively charged chitosan and the negatively charged of lecithin (Taner et al. 2014). Under acidic conditions, chitosan is protonated with a positive charge in the amino groups (NH_3^+) and phosphates of lecithin are attached by electrostatic forces, creating a network (Fig. 1). The symmetric group (COO^-) was assigned at 1464 cm^{-1} and the peak of asymmetric stretching vibration of phosphate groups was identified at 1156.88 cm^{-1} . This last binding is a reflection of the limited movement of the acyl chains of de CH_2 groups between lecithin, TPP and chitosan (Deygen and Kudryashova 2016). The bands located at 1381.68 and 1343.68 cm^{-1} are represented by $\text{C}-\text{O}-\text{H}$ bending (Tahira et al. 2019). A $\text{P}-\text{O}$ bond was observed in lower region at 897.08 cm^{-1} . Consistent with the reports of authors such as Vinodhini et al. (2017), the presence of OH^- and NH stretching vibrations was observed in the broad peak at 3600 cm^{-1} . The peak at 716.78 cm^{-1} remained constant compared to pure lecithin, as reported by Michał et al. (2015).

X-ray diffraction

XRD patterns were obtained to identify the crystalline phase structure of the material. Jayakrishnan and Ramesan (2016) recognized this practice as a nondestructive routine analytical technique. XRD can provide the degree of crystallinity in polymers (Nasrazadani and Hassani 2016). X-ray diffractograms of chitosan nano-onions are shown in figure 3. Saravanan and Ramasamy (2016) reported for pure chitosan characteristic peaks around 10° and 20° - 30° , and they defined it as a semi-crystalline structure. X-ray diffraction studies show that the polymorphic form of chitosan disappears when CSNO is produced, resulting in a more defined form. The peaks of CSNO were located at 18.05° and 23.03° . The first peak had a right displacement, attributed to the presence of lecithin bonded to the chitosan's surface. The second peak corresponded to the semi-crystalline structure of chitosan in which lecithin was incorporated. Dai et al. (2017) reported that lecithin, like chitosan, is amorphous as a result of its lack of crystallinity. Investigations made by Fan et al. (2019) about the production of these kinds of materials in terms of XRD correspond to the chitosan-TPP-lecithin nanosystem.

Scanning electron microscopy, energy-dispersive X-ray spectrophotometer, and specific surface area

The morphology of CSNO was observed by using SEM (shown in Figure 4). The micrographs were taken with 2000x amplification using a

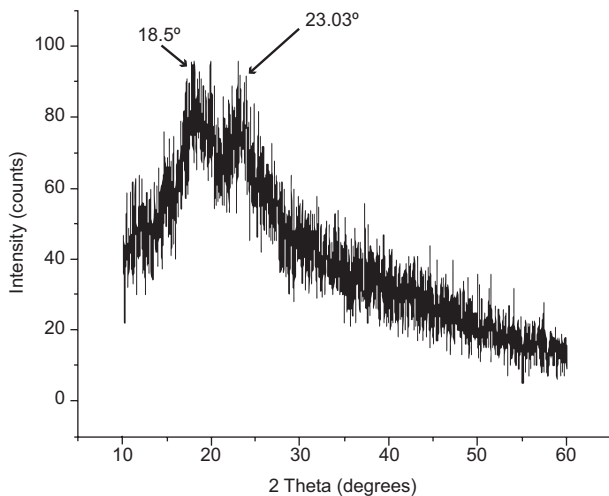


Fig. 3. X-Ray diffractogram of chitosan nano-onions (CSNO).

10- μm scale. CSNO exhibited a package-aggregated form with concave surfaces of several sizes. The same morphology was shown in some research reported by Tamura and Ichikawa (1997), Michał et al. (2015), Wang et al. (2017) and Pérez-Ruiz et al. (2018). The robustness of the particles was attributed to the presence of lecithin. Other particles such as flakes, similar to the original chitosan, were observed; in these cases the presence of not converted chitosan nano-onions was suggested. The morphology suggests a flat possible surface of active sites for adsorption of pollutants.

The combination of SEM and EDS allows for an elemental analysis performed on different microscopic sections of the samples (Nasrazadani and Hassani 2016). In this case, **figure 5** represent the spectra of the CSNO sample's EDS. The spectra indicates the presence of P and O distributed in the sample. It was also proven that the sample contains a small amount of Na. The EDS spectrum (**Fig. 5b**)

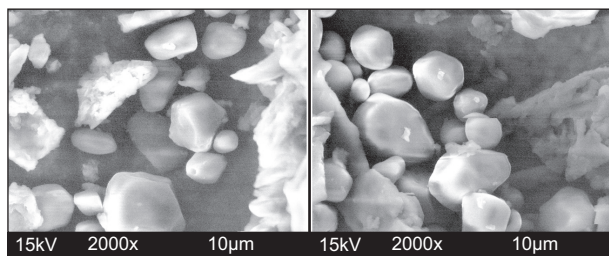


Fig. 4. Scanning electron microscope images of chitosan nano-onions at 2000x.

states the presence of C, N, O, Na, and P with a weight percentage of 47.10, 5.55, 26.23, 1.17, and 19.94 %, respectively. The EDS spectrum does not exhibit extra peaks, another confirmation of the crosslinking between lecithin and TPP in chitosan during the formation of CSNO. Additionally, it was confirmed that the sample was handled properly for reading, since no foreign element resulted in the analysis of elements.

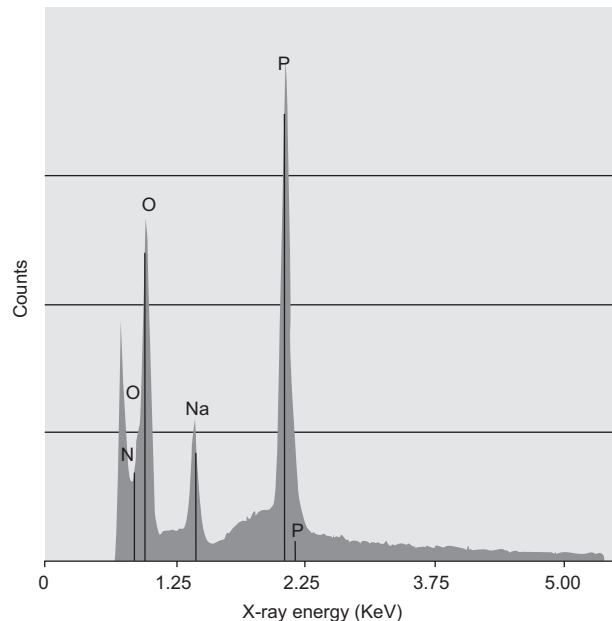


Fig. 5. Elemental analysis of chitosan nano-onions (CSNO).

CSNO presented a specific superficial area of $1.4 \text{ m}^2 \text{ g}^{-1}$. Due to their small size, the surface area was corroborated. The external superficial area was not only applied for water treatment, since other researchers used this property for energy storage applications (Zeiger et al. 2016). According to Khajeh et al. (2013), the high specific surface area, the adsorption and chemical activities, the location of atoms on the surface, the lack of internal diffusion resistance, and high surface binding energy are important factors that influence the adsorption process in the aqueous environment. The superficial area is a very important parameter in the formulation of CSNO. **Figure 6** shows the N_2 adsorption-desorption isotherm. The CSNO show a hysteresis loop of type-IV isotherms with the sudden increase at $P/P_0 = 0.4-0.6$ and exhibit a pore size distribution

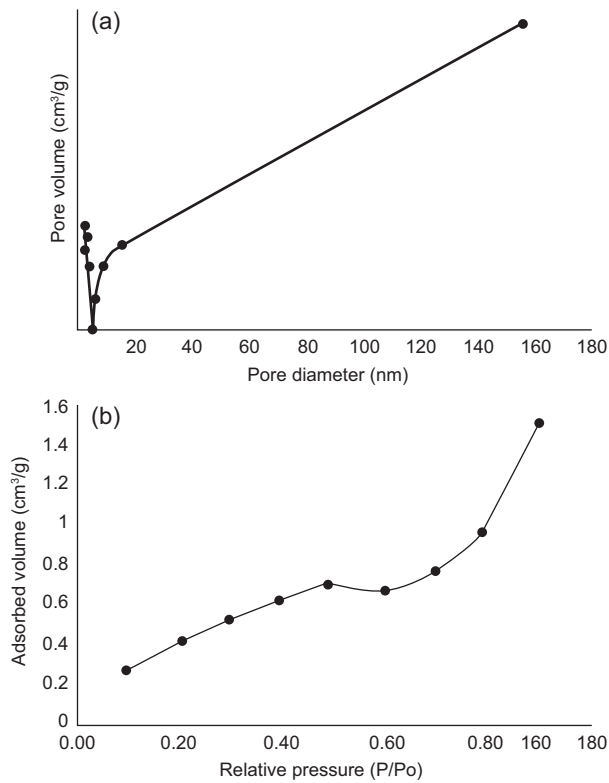


Fig. 6. (a) Pore distribution and (b) nitrogen adsorption and desorption isotherm of chitosan nano-onions (CSNO).

of 5-18 nm. Other authors such as Li et al. (2011) presented similar results by using chitosan-modified iron nanoparticles.

Transmission electron microscopy and dynamic light scattering

High resolution characterization plays an important role in the understanding of relationships between microstructure and materials properties and underpins the development of new materials (Liu et al. 2019). Factors that control the properties of nanoadsorbents are the size of particles, specific surfaces, agglomeration sites, chemical composition, crystalline structure, and solubility (Krstić et al. 2018). **Figure 7** corresponds to the CSNO analysis performed with SEM. These images (**Fig. 5a**) presented nano-onions congregated in a unique structure including a number of overlapping nanotubes along the sample. In **figure 7c** the formation of concentric multilayers was accentuated with a homogeneous interplanar spacing of 0.393 nm between each layer and with a hexagonal arrangement. In addition, a hollow was shown.

The diameter of CSNO measured by TEM was in the range of 21-23 nm. In **figure 5b, d** the arrangement of planes can be appreciated. Authors such as Lange et al. (2003), He et al. (2019) and Gindl-Altmutter et al. (2019) have reported approximately the same layer distance for carbon nano-onions. On the other hand, all the results shown by TEM were a proof of the formation of nanostructures.

The DLS of CSNO indicated that the hydrodynamic diameter of the particles was between 400 and 700 nm, with an average of 442.5 nm, a PDI of 0.532 and a zeta potential of 31.9 mV. In their work, Mahdieh et al. (2012) published diameter

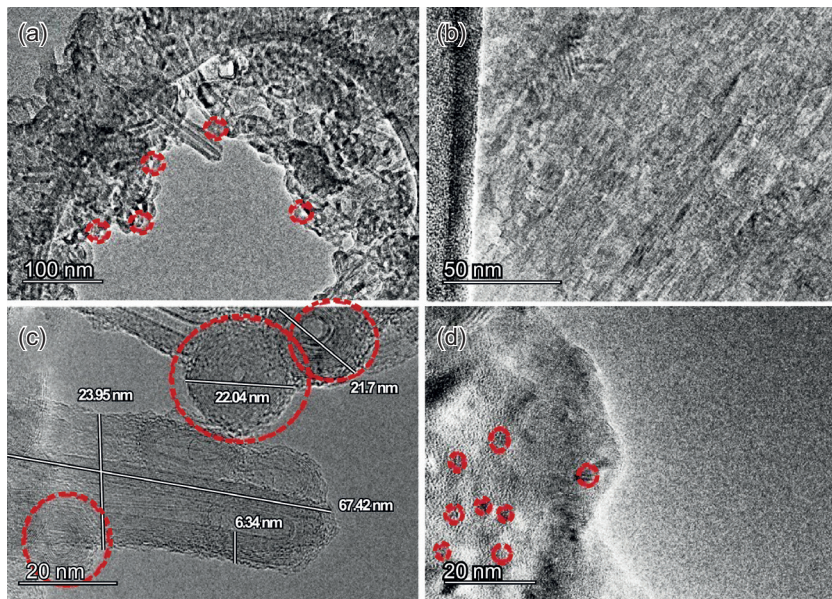


Fig. 7. Transmission electron micrographs of chitosan nano-onions (CSNO).

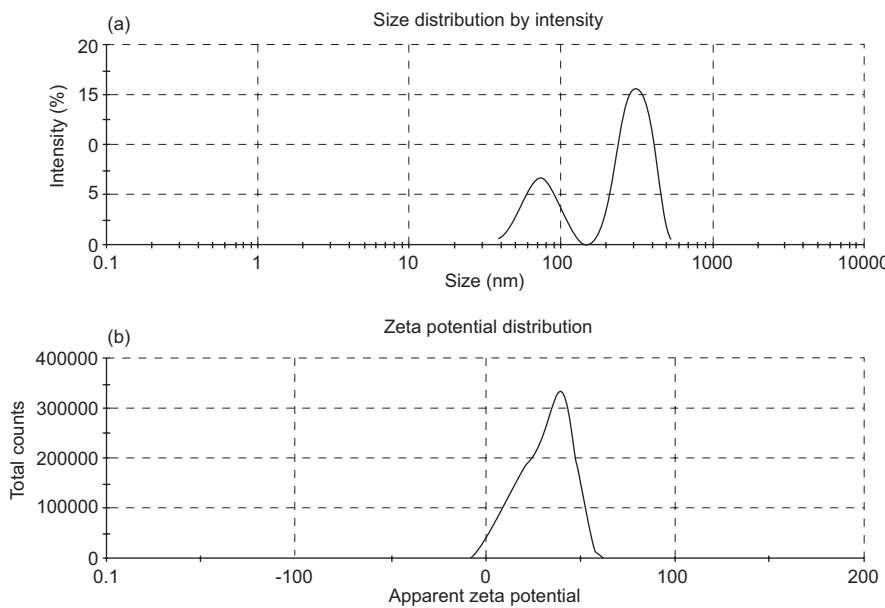


Fig. 8. (a) Hydrodynamic diameter and (b) zeta potential distribution of chitosan nano-onions (CSNO).

intervals of 150-400 nm for nanotubes and CSNO used for biomedical applications. Adsorption of phenol onto chitosan hydrogel scaffold modified with carbon nanotubes reaches the maximum capacity of 404.2 mg g^{-1} at 30°C , a higher value than the one given in this work. The disparity of size between DLS and TEM was related with the sample preparation. In TEM, the sample was used in solid state while in DLS an aqueous solution was used resulting in a hydrodynamic diameter (Maguire et al. 2018).

The zeta potential is an absolute value which describes the intensity of an electric camp (Fig. 8). If it is above 30 mV, this indicates a stable colloidal dispersion that has the ability to attract other molecules of interest to the polymeric matrix. If it is below 30 mV, agglomeration effects occur between the same particles (Kašpar et al. 2013). In this case (zeta potential = 31.9 mV) the results suggested the trapping of other particles, signifying a high probability of being used for adsorption purposes. In addition, the PDI was a related parameter which confirmed the information of the zeta potential value. PDI is the measurement of the degree of dispersion given in a polymer sample, which in this analysis had a value of 0.532. Masarudin et al. (2015) reported that in PDIs > 0.5 , nanoparticles tend to aggregate.

CONCLUSIONS

The production of CSNO using a simple method and a natural and environmentally friendly chitosan

source (shrimp waste) was possible. The obtained CSNO were considered self-organized structures resulting from the electrostatic interaction of chitosan and lecithin. In addition, chitosan nanotubes were also produced. The characterization made by XRD showed an amorphous structure. FTIR confirmed the addition of phosphate groups of lecithin by the appearance of a new band peak at 1752.13 cm^{-1} . The nano-onions average size obtained by DLS was between 400 to 700 nm, while by using TEM it resulted in a diameter between 20-25 nm and an interplanar distance of 0.393 nm. The PDI and the zeta potential value were indicators of a stable dispersion with capacity to entrap other molecules. CSNO could be used as adsorbents of pollutants in water solutions in further experiments. The change in shape and surface of nanoparticles is a key factor that may be applied in specific fields.

ACKNOWLEDGMENTS

This work was sponsored by Instituto Tecnológico de Sonora through projects PROFAPI_2019_0133, PROFAPI_2022_0490, and PROFAPI_2022_0512.

REFERENCES

Abd El-Aziz M.E., Morsi S.M.M., Salama D.M., Abdel-Aziz M.S., Abd Elwahed M.S., Shaaban E.A. and Youssef A.M. (2019). Preparation and characterization

of chitosan/polyacrylic acid/copper nanocomposites and their impact on onion production. *International Journal of Biological Macromolecules* 123, 856-865. <https://doi.org/10.1016/j.ijbiomac.2018.11.155>

Amiri M., Salehniya H. and Habibi-Yangjeh A. (2016). Graphitic carbon nitride/chitosan composite for adsorption and electrochemical determination of mercury in real samples. *Industrial and Engineering Chemistry Research* 55 (29), 8114-8122. <https://doi.org/10.1021/acs.iecr.6b01699>

Dai L., Sun C., Li R., Mao L., Liu F. and Gao Y. (2017). Structural characterization, formation mechanism and stability of curcumin in zein-lecithin composite nanoparticles fabricated by antisolvent co-precipitation. *Food Chemistry* 237, 1163-1171. <https://doi.org/10.1016/j.foodchem.2017.05.134>

De Toledo A.M.N., Silva N.C.C., Sato A.C.K. and Picone C.S.F. (2021). A comprehensive study of physical, antimicrobial and emulsifying properties of self-assembled chitosan/lecithin complexes produced in aqueous media. *Future Foods* 4, 1-7. <https://doi.org/10.1016/j.fufo.2021.100083>

Deygen I.M. and Kudryashova E.V. (2016). Effect of glycol chitosan on functional and structural properties of anionic liposomes. *Moscow University Chemistry Bulletin* 71 (3), 167-171. <https://doi.org/10.3103/s0027131416030044>

Divya K., Vijayan S., Nair S.J. and Jisha M.S. (2019). Optimization of chitosan nanoparticle synthesis and its potential application as germination elicitor of *Oryza sativa* L. *International Journal of Biological Macromolecules* 124, 1053-1059. <https://doi.org/10.1016/j.ijbiomac.2018.11.185>

Dou J., Gan D., Huang Q., Liu M., Chen J., Deng F., Zhu X., Wen Y., Zhang X. and Wei Y. (2019). Functionalization of carbon nanotubes with chitosan based on MALI multicomponent reaction for Cu²⁺ removal. *International Journal of Biological Macromolecules* 136, 476-485. <https://doi.org/10.1016/j.ijbiomac.2019.06.112>

Fan J., Chen Q., Li J., Wang D., Zheng R., Gu Q. and Zhang Y. (2019). Preparation and dewatering property of two sludge conditioners chitosan/AM/AA and chitosan/AM/AA/DMDAAC. *Journal of Polymers and the Environment* 27 (2), 275-285. <https://doi.org/10.1007/s10924-018-1342-0>

Frank L.A., Onzi G.R., Morawski A.S., Pohlmann A.R., Guterres S.S. and Contri R.V. (2020). Chitosan as a coating material for nanoparticles intended for biomedical applications. *Reactive and Functional Polymers* 147, 104459. <https://doi.org/10.1016/j.reactfunctpolym.2019.104459>

Gindl-Altmutter W., Köhnke J., Unterweger C., Gierlinger N., Keckes J., Zalesak J. and Rojas O.J. (2019). Lignin-based multiwall carbon nanotubes. *Composites Part A: Applied Science and Manufacturing* 121, 175-179. <https://doi.org/10.1016/j.compositesa.2019.03.026>

Goycoolea F.M., Valle-Gallego A., Stefani R., Menchicchi B., David L., Rochas C., Santander-Ortega M.J. and Alonso M.J. (2012). Chitosan-based nanocapsules: Physical characterization, stability in biological media and capsaicin encapsulation. *Colloid and Polymer Science* 290 (14), 1423-1434. <https://doi.org/10.1007/s00396-012-2669-z>

Guo M., Wang J., Wang C., Strong P.J., Jiang P., Ok Y.S. and Wang H. (2019). Carbon nanotube-grafted chitosan and its adsorption capacity for phenol in aqueous solution. *Science of The Total Environment* 682, 340-347. <https://doi.org/10.1016/j.scitotenv.2019.05.148>

He C., Shi L., Lou S., Liu B., Zhang W. and Zhang L. (2019). Synthesis of spherical magnetic calcium modified chitosan micro-particles with excellent adsorption performance for anionic-cationic dyes. *International Journal of Biological Macromolecules* 128, 593-602. <https://doi.org/10.1016/j.ijbiomac.2019.01.189>

Jayakrishnan P. and Ramesan M. (2016). Synthesis, characterization and properties of poly (vinyl alcohol)/chemically modified and unmodified pumice composites. *Journal of Chemical and Pharmaceutical Sciences* 5 (1), 97-104.

Kašpar O., Jakubec M. and Štěpánek F. (2013). Characterization of spray dried chitosan-TPP microparticles formed by two- and three-fluid nozzles. *Powder Technology* 240, 31-40. <https://doi.org/10.1016/j.powtec.2012.07.010>

Khajeh M., Laurent S. and Dastafkan K. (2013). Nano-adsorbents: Classification, preparation, and applications (with emphasis on aqueous media). *Chemical Reviews* 113 (10), 7728-7768. <https://doi.org/10.1021/cr400086v>

Krstić V., Urošević T. and Pešovski B. (2018). A review on adsorbents for treatment of water and wastewater containing copper ions. *Chemical Engineering Science* 192, 273-287. <https://doi.org/10.1016/j.ces.2018.07.022>

Kwamman Y., Mahisanunt B., Matsukawa S. and Klinke-sorn U. (2016). Evaluation of electrostatic interaction between lysolecithin and chitosan in two-layer tuna oil emulsions by nuclear magnetic resonance (NMR) spectroscopy. *Food Biophysics* 11 (2), 165-175. <https://doi.org/10.1007/s11483-016-9427-6>

Lange H., Sioda M., Huczko A., Zhu Y.Q., Kroto H.W. and Walton D.R.M. (2003). Nanocarbon production by arc discharge in water. *Carbon* 41 (8), 1617-1623. [https://doi.org/10.1016/S0008-6223\(03\)00111-8](https://doi.org/10.1016/S0008-6223(03)00111-8)

Li Y., Yao L., Liu S., Zhao J., Ji W. and Chak-Tong A. (2011). Cs-modified iron nanoparticles encapsulated

in microporous and mesoporous SiO_2 for CO_x -free H_2 production via ammonia decomposition. *Catalysis Today* 160 (1), 79-86. <https://doi.org/10.1016/j.cat.2010.02.066>

Lin W. (2015). Introduction: Nanoparticles in medicine. *Chemical Reviews* 115 (19), 10407-10409. <https://doi.org/10.1021/acs.chemrev.5b00534>

Liu J., Lozano-Pérez S., Karamched P., Holter J., Wilkinson A.J. and Grovenor C.R.M. (2019). Forescattered electron imaging of nanoparticles in scanning electron microscopy. *Materials Characterization* 155, 1-9. <https://doi.org/10.1016/j.matchar.2019.109814>

Magnuson B.A., Jonaitis T.S. and Card J.W. (2011). A brief review of the occurrence, use, and safety of food-related nanomaterials. *Journal of Food Science* 76 (6), R126-R133. <https://doi.org/10.1111/j.1750-3841.2011.02170.x>

Maguire C.M., Rösslein M., Wick P. and Prina-Mello A. (2018). Characterisation of particles in solution – A perspective on light scattering and comparative technologies. *Science and Technology of Advanced Materials* 19 (1), 732-745. <https://doi.org/10.1080/14686996.2018.1517587>

Mahdieu Z.M., Mottaghitalab V., Piri N. and Haghie A.K. (2012). Conductive chitosan/multi walled carbon nanotubes electrospun nanofiber feasibility. *Korean Journal of Chemical Engineering* 29 (1), 111-119. <https://doi.org/10.1007/s11814-011-0129-y>

Masarudin M.J., Cutts S.M., Evison B.J., Phillips D.R. and Pigram P.J. (2015). Factors determining the stability, size distribution, and cellular accumulation of small, monodisperse chitosan nanoparticles as candidate vectors for anticancer drug delivery: Application to the passive encapsulation of [(14)C]-doxorubicin. *Nanotechnology, Science and Applications* 8, 67-80. <https://doi.org/10.2147/nsa.s91785>

Mattu C., Li R. and Ciardelli G. (2013). Chitosan nanoparticles as therapeutic protein nanocarriers: The effect of pH on particle formation and encapsulation efficiency. *Polymer Composites* 34 (9), 1538-1545. <https://doi.org/10.1002/pc.22415>

Michał W., Ewa D. and Tomasz C. (2015). Lecithin-based wet chemical precipitation of hydroxyapatite nanoparticles. *Colloid and Polymer Science* 293 (5), 1561-1568. <https://doi.org/10.1007/s00396-015-3557-0>

Mykhailiv O., Zubyk H. and Plonska-Brzezinska M.E. (2017). Carbon nano-onions: Unique carbon nanostructures with fascinating properties and their potential applications. *Inorganica Chimica Acta* 468, 49-66. <https://doi.org/10.1016/j.ica.2017.07.021>

Nasrazadani S. and Hassani S. (2016). Modern analytical techniques in failure analysis of aerospace, chemical, and oil and gas industries. In: *Handbook of materials failure analysis with case studies from the oil and gas industry* (Makhlouf A.S.H. and Aliofkazraei M., Eds.). Elsevier, Amsterdam, Nederlands, 39-54. <https://doi.org/10.1016/B978-0-08-100117-2.00010-8>

Pérez-Ruiz A.G., Ganem A., Olivares-Corichi I.M. and García-Sánchez J.R. (2018). Lecithin-chitosan-TPGS nanoparticles as nanocarriers of (-)-epicatechin enhanced its anticancer activity in breast cancer cells. *RSC Advances* 8 (61), 34773-34782. <https://doi.org/10.1039/c8ra06327c>

Peters R.J.B., Bouwmeester H., Gottardo S., Amenta V., Arena M., Brandhoff P., Marvin H.J.P., Mech A., Moniz F.B., Pesudo L.Q., Rauscher H., Schoonjans R., Undas A.K., Vettori M.V., Weigel S. and Aschberger K. (2016). Nanomaterials for products and application in agriculture, feed and food. *Trends in Food Science and Technology* 54, 155-164. <https://doi.org/10.1016/j.tifs.2016.06.008>

Plonska-Brzezinska M.E. (2019). Carbon nano-onions: A review of recent progress in synthesis and applications. *ChemNanoMat* 5 (5), 568-580. <https://doi.org/10.1002/cnma.201800583>

Sánchez-Duarte R.G., Sánchez-Machado D.I., López-Cervantes J. and Correa-Murrieta M.A. (2012). Adsorption of allura red dye by cross-linked chitosan from shrimp waste. *Water Science and Technology* 65, 618-623. <https://doi.org/10.2166/wst.2012.900>

Santhosh C., Velmurugan V., Jacob G., Jeong S.K., Grace A.N. and Bhatnagar A. (2016). Role of nanomaterials in water treatment applications: A review. *Chemical Engineering Journal* 306, 1116-1137. <https://doi.org/10.1016/j.cej.2016.08.053>

Saravanan A. and Ramasamy R. (2016). Chitosan-maghemite- LiClO_4 – A new green conducting superparamagnetic nanocomposite. *Journal of Polymer Research* 23 (174), 1-11. <https://doi.org/10.1007/s10965-016-1072-8>

Shi J., Votruba A.R., Farokhzad O.C. and Langer R. (2010). Nanotechnology in drug delivery and tissue engineering: From discovery to applications. *Nano Letters* 10 (9), 3223-3230. <https://doi.org/10.1021/nl102184c>

Singh V. (2018). Natural source derived carbon nano-onions as electrode material for sensing applications. *Diamond and Related Materials* 87, 202-207. <https://doi.org/10.1016/j.diamond.2018.06.007>

Sonvico F., Cagnani A., Rossi A., Motta S., Di Bari M.T., Cavatorta F., Alonso M.J., Deriu A. and Colombo P. (2006). Formation of self-organized nanoparticles by lecithin/chitosan ionic interaction. *International Journal of Pharmaceutics* 324 (1), 67-73. <https://doi.org/10.1016/j.ijpharm.2006.06.036>

Souza M.P., Vaz A.F.M., Correia M.T.S., Cerqueira M.A., Vicente A.A. and Carneiro-da-Cunha M.G. (2014).

Quercetin-loaded lecithin/chitosan nanoparticles for functional food applications. *Food and Bioprocess Technology* 7 (4), 1149-1159. <https://doi.org/10.1007/s11947-013-1160-2>

Stoica-Guzun A., Dobre L., Stroescu M. and Jipa I. (2010). Fourier transform infrared (FTIR) spectroscopy for characterization of antimicrobial films containing chitosan. Fourier transform infrared (FTIR) spectroscopy for characterization of antimicrobial films containing chitosan. *Journal Analele Universității din Oradea, Fascicula: Ecotoxicologie, Zootehnie și Tehnologii de Industrie Alimentară*, 815-822.

Suárez-Martínez I., Grobert N. and Ewels C.P. (2012). Nomenclature of sp2 carbon nanoforms. *Carbon* 50 (3), 741-747. <https://doi.org/10.1016/j.carbon.2011.11.002>

Tahira I., Aslam Z., Abbas A., Monim-ul-Mehboob M., Ali S. and Asghar A. (2019). Adsorptive removal of acidic dye onto grafted chitosan: A plausible grafting and adsorption mechanism. *International Journal of Biological Macromolecules* 136, 1209-1218. <https://doi.org/10.1016/j.ijbiomac.2019.06.173>

Tamura T. and Ichikawa M. (1997). Effect of lecithin on organogel formation of 12-hydroxystearic acid. *Journal of the American Oil Chemists Society* 74 (5), 491-495. <https://doi.org/10.1007/s11746-997-0170-5>

Taner G., Yeşilöz R., Özkan Vardar D., Şenyiğit T., Özer Ö., Degen G.H. and Başaran N. (2014). Evaluation of the cytotoxic and genotoxic potential of lecithin/chitosan nanoparticles. *Journal of Nanoparticle Research* 16 (2), 2220. <https://doi.org/10.1007/s11051-013-2220-2>

Tran T.H., Nguyen T.D., Poudel B.K., Nguyen H.T., Kim J.O., Yong C.S. and Nguyen C.N. (2015). Development and evaluation of artesunate-loaded chitosan-coated lipid nanocapsule as a potential drug delivery system against breast cancer. *AAPS PharmSciTech* 16 (6), 1307-1316. <https://doi.org/10.1208/s12249-015-0311-3>

Valencia M.S., Silva Júnior M.F., Xavier-Júnior F.H., Veras B.O., Albuquerque P.B.S., Borba E.F.O., Silva T.G., Xavier V.L., Souza M.P. and Carneiro-da-Cunha M.G. (2021). Characterization of curcumin-loaded lecithin-chitosan bioactive nanoparticles. *Carbohydrate Polymer Technologies and Applications* 2, 100119. <https://doi.org/10.1016/j.carpta.2021.100119>

Villegas-Peralta Y., Correa-Murrieta M.A., Meza-Escalante E.R., Flores-Aquino E., Álvarez-Sánchez J. and Sánchez-Duarte R.G. (2019). Effect of the preparation method in the size of chitosan nanoparticles for the removal of allura red dye. *Polymer Bulletin* 76 (9), 4415-4430. <https://doi.org/10.1007/s00289-018-2601-x>

Vinodhini P.A., Sangeetha K., Gomathi T., Sudha P.N., Venkatesan J. and Anil S. (2017). FTIR, XRD and DSC studies of nanochitosan, cellulose acetate and polyethylene glycol blend ultrafiltration membranes. *International Journal of Biological Macromolecules* 104, 1721-1729. <https://doi.org/10.1016/j.ijbiomac.2017.03.122>

Wang S., Shi Y., Tu Z., Zhang L., Wang H., Tian M. and Zhang N. (2017). Influence of soy lecithin concentration on the physical properties of whey protein isolate-stabilized emulsion and microcapsule formation. *Journal of Food Engineering* 207, 73-80. <https://doi.org/10.1016/j.jfoodeng.2017.03.020>

Wang Y., Jou C. and Yang M. (2011). Effect of quaternized chitosan on the fusion efficiency and cytocompatibility of liposomes. *Journal of Polymer Research* 19 (1), 9755. <https://doi.org/10.1007/s10965-011-9755-7>

Yousfan A., Rubio N., Natouf A.H., Daher A., Al-Kafry N., Venner K. and Kafa H. (2020). Preparation and characterisation of PHT-loaded chitosan lecithin nanoparticles for intranasal drug delivery to the brain. *RSC Advances* 10 (48), 28992-29009. <https://doi.org/10.1039/d0ra04890a>

Zeiger M., Jäckel N., Mochalin V.N. and Presser V. (2016). Review: Carbon onions for electrochemical energy storage. *Journal of Materials Chemistry A* 4 (9), 3172-3196. <https://doi.org/10.1039/c5ta08295a>